Gd-EOB-DTPA-enhanced MRI in cirrhotic liver in rats; with reference to transporter activity and morphological change of bile canaliculi

N. Tsuda[1], and O. Matsui[2]

[1]Bayer Yakuhin, Ltd, Osaka, Osaka, Japan, [2]Kanazawa University Graduate School of Medical Science, Kanazawa, Kanazawa, Japan

Introduction

Gd-EOB-DTPA is useful for differentially diagnosing benign and malignant liver tumors. After intravenous injection, it partially accumulates in hepatocytes followed by excretion into the bile under the regulation of various transporters. Liver cirrhosis, an end stage event of chronic liver disease, leads to a multi-step process of hepatocarcinogenesis. As a result, cirrhosis is often observed in the surrounding liver in hepatocellular carcinoma (HCC). However, it is well known that signal enhancement of the cirrhotic liver in the hepatobiliary phase of Gd-EOB-DTPA-enhanced MRI is weak in comparison with normal liver, resulting in deterioration of the detectability of HCCs. Therefore, clarifying the mechanism of weaker enhancement in cirrhotic liver is considered to be important to improve the diagnostic ability of Gd-EOB-DTPA-enhanced MRI.The purpose of this study was to analyze the difference of signal intensity on Gd-EOB-DTPA-enhanced MRI between normal and cirrhotic livers in rats in correlation with the expressions of the transporters of Gd-EOB-DTPA and the morphopathological change of bile canaliculi and to discuss the possible mechanisms of the signal profile of Gd-EOB-DTPA-enhanced MRI in cirrhotic livers.

Methods

Fifteen male Wistar rats received 0.03% thioacetamide solution to induce liver cirrhosis for 12 weeks (TAA group) and were divided into 3 groups as follows: first group for MRI (n=7), second group for PCR (n=5), third group for morphological analysis (n=3). Rats were subjected to Gd-EOB-DTPA (Primovist, Bayer AG)-enhanced MRI with 2D-FLASH; TR/ TE = 101/2.9 msec, nearly opposed-phase, flip angle 90º using a 1.0 T clinical imager under anesthesia with pentobarbital and urethane (n=7). The field-of-view was 180 × 90 mm with a matrix of 256 × 128. Slice thickness was 5.5 mm and slice number was 12. The excitation number was 1 and the actual acquisition time was 6.4 sec. Gd-EOB-DTPA (0.025 mmol Gd/kg) was manually injected into the tail vein. Nineteen images, including 3 precontrast measurements, were taken at intervals of 12 sec up to 3 min after injection of the contrast agent, which was injected immediately after acquisition of the third measurement. Subsequently, seven MR images were acquired 5, 10, 15, 20, 30, 45 and 60 min after injection. The signal intensity (SI) of the liver was measured for each MR image, and relative enhancement (RE) was calculated. We combined a laser capture microdissection (LCM) technique with real-time reverse transcription polymerase chain reaction (RT-PCR) to compare the transporter activity between cirrhotic and normal liver. LCM was used to isolate homogeneous cells under microscopic observation. RT-PCR was used for a quantitative analysis of transporter activity. Five rats from each group were used for RT-PCR examination. Livers were removed, frozen and stored at -80 °C. Whole liver was divided into15 blocks, and 15 slides of 15 μm for each block were prepared. Three slides (slide number: 1, 8, 15) were stained with hematoxylin and eosin (HE) to identify liver cirrhosis. Fibrosis in the TAA group was identified by Sirius red staining. As a control, slides prepared from normal rats were used. Three rats from each group were used for morphological analysis. The transmission electron microscopy (TEM) and scanning electron microscopy (SEM) were performed.

Results and Discussion

Typical T1-weighted images of liver and kidney before, 3 min (hepatobiliary phase for rats) and 30 min (near baseline) after Gd-EOB-DTPA injection in both groups are shown in Figure 1. Signal enhancement of the liver in the TAA group was weak in comparison with the control group, and the RE in the liver of the TAA group was significantly lower than that of the TAA group (0-15 min: $p < 0.01$, 20 min: $p < 0.05$). On the other hand, signal enhancement of the kidney in the TAA group was almost equivalent to that in the control group, and there was no significant difference in the RE in the kidney between groups; however, the RE in the kidney of the TAA group seemed to be higher in the early phase (1.4-3 min), and then lower in the late phase (10-30 min) than that of the control group. Therefore, it was suggested that there was no massive difference in Gd-EOB-DTPA elimination via the hepatobiliary transport system between normal and cirrhotic livers, though there may be a quantitative problem in the evaluation of renal excretion by the signal-intensity curve of Gd-EOB-DTPA-enhanced MRI. We hypothesized as follows: the elimination system via bile may be activated in the cirrhotic liver in order to prevent the accumulation of xenobiotic substance (such as Gd-EOB-DTPA) in hepatocytes. To verify this hypothesis, we examined the transporter activities of both groups.

We succeeded in extracting RNA from each sample, and compared oatp1 and mrp2 activity in both groups. The oatp1 activity was as follows: 2.17 ± 0.71 (TAA group), 2.58 ± 0.35 (control group). The oatp1 activity in the TAA group slightly decreased in comparison with the control group, although there was no significant difference between groups (Fig 2). On the other hand, mrp2 activity was as follows: 3.37 ± 1.04 (TAA group) and 0.93 ± 0.34 (control group). The mrp2 in the TAA group was significantly higher than in the control group ($p<0.01$). It was found that liver cirrhosis would slightly interfere with the uptake of Gd-EOB-DTPA mediated by oatp1 and promote the elimination of Gd-EOB-DTPA mediated by mrp2; accordingly, the combination of oatp1 down-regulation and mrp2 up-regulation, especially the latter, would lead to a significant signal loss on Gd-EOB-DTPA-enhanced MRI.

The ultrastructure of normal and cirrhotic liver was compared by SEM and TEM (Fig 3, 4). Wherever two hepatocytes adhered, a tubular space known as a bile canaliculus was observed; however, several changes in the size and structure of bile canaliculi were detected between groups. Branching bile canaliculi were observed in normal and cirrhotic liver by SEM; however, the distribution of microvilli increased in cirrhotic liver in comparison with normal liver. In particular, thin elongated microvilli and aggregation of microvilli were detected in the cirrhotic liver, and dilated bile canaliculi formed a space filled with bile. The surface of normal hepatocytes was smooth, whereas cirrhotic liver showed irregular surface contours and many pores like a fenestra formed by vacuolar degeneration with adiposis. In the TEM view, regular distribution of microvilli was identified in normal liver; however, it was found that dilated canaliculi were often observed in cirrhotic liver, and that thick short microvilli appeared in cirrhotic liver. Moreover, pre-interdigitations of the plasma membranes of two adherent cells in cirrhotic liver was sealed at each end by tight junctions. As far as we reviewed, there had been no report evaluating the functional aspect of these morphological changes of bile canaliculi. However, we supposed that these changes would indicate increased bile elimination activity in the cirrhotic liver, and would play an important role in the promoted elimination of Gd-EOB-DTPA. Consequently, it was thought that Gd-EOB-DTPA could not accumulate in hepatocytes due to highly activated elimination mediated by mrp2. In addition, the highly activated elimination system in bile canaliculi may induce the reduction of signal enhancement of cirrhotic liver on Gd-EOB-DTPA-enhanced MRI.

Figure 1

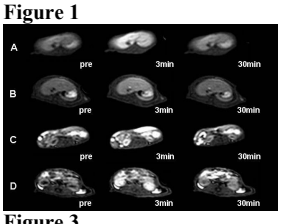

Figure 2

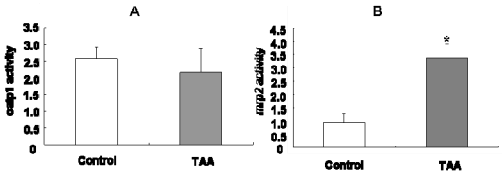

Figure 3

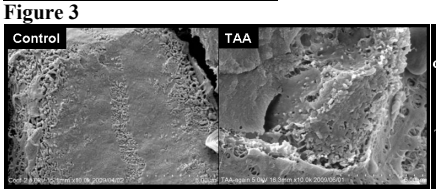

Figure 4